Similar Solutions of the Mean Velocity, Turbulent Energy and Length Scale Equation

H. Vollmers* and J. C. Rotta†
Deutsche Forschungs- und Versuchsanstalt für Luftp und Raumfahrt E. V., Aerodynamische Versuchsanstalt, Göttingen, W. Germany

A semiempirical approximation of the equations for second order correlations and moments was quantitatively investigated. The resulting partial differential equations for mean velocity, turbulent kinetic energy and length scale are supposed to be valid for plane and axisymmetric free as well as bounded turbulent flows. They were converted into ordinary differential equations by means of similarity transformations for six different flow cases (plane free jet, plane asymptotic wake, free mixing layer, plane channel flow, axisymmetric free jet, axisymmetric pipe flow) and then solved numerically. The values of the coefficients introduced for the closure of the equations were determined from investigations of the dependence of the solutions on them and by comparison with experimental results. A single set of coefficients was obtained, which reproduces the measurements of mean velocity for all six treated cases and the decay of homogeneous turbulence with satisfactory agreement.

I. Introduction

TURBULENT fluid flow is accepted to be a continuous motion governed by the Navier-Stokes equations. Because of the nonlinear character of the equations, the general solution of the Navier-Stokes equations can be obtained neither analytically nor numerically with the present-day computers. Therefore, prediction methods for engineering purposes are based on statistical formulations of the equations, for which some empirical closure assumptions have to be introduced. The oldest methods, in which the theory is combined with empirical approaches, are Boussinesq's eddy viscosity concept and Prandtl's mixing length formula. Although these relations describe the mean velocity field remarkably well for many cases, the main disadvantage is, among other shortcomings, that empirical assumptions are required for a field quantity, namely the eddy viscosity and the mixing length, respectively. This means, the empirical assumptions are related to the boundary conditions of the flow and are thus to be adjusted for each individual flow case. The essential motivation of current work is to develop computation methods, in which the empirical input consists of a number of coefficients rather than field quantities. These coefficients may be considered to be universally valid to some extent, such that the methods can be applied to a greater class of flows with the same values for the coefficients. The basic ideas of such methods and the progress attained are reviewed by Bradshaw,[1] Mellor and Herring,[2] Launder and Spalding,[3] Rotta,[4] and Reynolds.[5]

The present method is characterized in describing the flowfield by the mean velocity, turbulent kinetic energy and turbulent length scale. The objective of the present work is to achieve numerical solutions for various flow cases, to compare the results with experimental data available from the literature, and to determine a set of the coefficients, which yields best agreement between computed and experimental results for many cases. For this purpose similar solutions for the partial differential equations have been computed for six different flow cases: 1) The free plane jet in a fluid at rest, 2) the asymptotic plane wake, 3) the free mixing layer, 4) the fully developed plane flow in a channel, 5) the free round jet in a fluid at rest, and 6) the fully developed axisymmetric flow in a pipe.

Here, 'similar' solutions are defined as those for which the distributions of the dependent variables, which are functions of x and y, differ from each other only by scale functions of x. Therefore, in the case of such similar solutions, the distributions of mean velocity, turbulent energy, and length scale at all values of x can be made congruent, if they are plotted in coordinates which have been made dimensionless with reference to the scale functions. From the mathematical point of view, the similar solutions have the advantage that the partial differential equations reduce to ordinary differential equations. This approach is more precise than solving the partial differential equations with a finite difference procedure, which starts with some chosen initial distributions and is continued until asymptotic solutions are obtained. When many parameter variations have to be calculated, the solution of the ordinary differential equations is less expensive than that of the initial value problem.

II. Governing Equations

The equations are valid for constant density fluid flows which are stationary and plane or axisymmetric (without swirl) with respect to mean values. They contain the usual boundary-layer approximations. The Reynolds numbers are supposed to be high such that the kinematic viscosity does not appear explicitly. A detailed deduction and discussion of the equations was given by Rotta.[6,7] Only the transport equation for the length scale will be treated here with respect to a refinement of the approximation for the production term.

The mean velocity field is represented by the components $\bar{u}$ and $\bar{v}$. The coordinate x is aligned with the main stream direction denoted by $\bar{u}$. The component $\bar{v}$ is either the second cartesian component or the radial component in cylindrical coordinate systems. Then y denotes the pertinent coordinate. Thus the continuity equation reads

$$\frac{\partial \bar{u}}{\partial x} + \frac{1}{y^j}\frac{\partial (y^j \bar{v})}{\partial y} = 0 \tag{1}$$

where $j=0$ for plane flows and $j=1$ for axisymmetric flows. The momentum equations reads

$$\rho\left(\bar{u}\frac{\partial \bar{u}}{\partial x} + \bar{v}\frac{\partial \bar{u}}{\partial y}\right) = \frac{1}{y^j}\frac{\partial (y^j \tau)}{\partial y} - \frac{\mathrm{d}\bar{p}}{\mathrm{d}x} \tag{2}$$

Presented as Paper 76-407 at the AIAA 9th Fluid and Plasma Dynamics Conference, San Diego, Calif., July 14-16; revision received Jan. 19, 1977.

Index categories: Jets, Wakes, and Viscid-Inviscid Flow Interactions; Nozzle and Channel Flow.

*Member of Staff.

†Deputy Director of Institute for Fluid Mechanics.

Because of the high Reynolds number approximation, the stress τ consists entirely of the Reynolds' stress $\tau = -\rho\overline{u'v'}$, where the accent denotes the fluctuating part of the quantities, and the overbars indicate time averages. The static pressure $\bar{p}$ is independent of y.

The transport equation for the turbulent energy per unit of mass, $E = (\overline{u'^2} + \overline{v'^2} + \overline{w'^2})/2$, is used in the form suggested by Prandtl[8]

$$\underset{\text{convection}}{\bar{u}\frac{\partial E}{\partial x} + \bar{v}\frac{\partial E}{\partial y}} = \underset{\text{dissipation}}{-c\frac{E^{3/2}}{L}} + \underset{\text{production}}{\frac{\tau}{\rho}\frac{\partial \bar{u}}{\partial y}} + \underset{\text{diffusion}}{\frac{k_q}{y^j}\frac{\partial}{\partial y}\left(y^j\sqrt{E}L\frac{\partial E}{\partial y}\right)} \tag{3}$$

and has been extended to axisymmetric flows. The variable L stands for the turbulent length scale defined below, and c and k_q are dimensionless coefficients. Equation (3) states that the rate of change of energy of a small volume of fluid, which is moving with the mean flow velocity (convection) is caused by conversion into heat (dissipation), by creation of new energy due to the work done by the rate of mean strain on the shear stress (production), and by transport of energy due to turbulent mixing (diffusion).

For the present investigation of self-similar flowfields the equation

$$\tau = \rho k\sqrt{E}L\frac{\partial \bar{u}}{\partial y} \tag{4}$$

with the constant coefficient k is supposed to be sufficient to relate the Reynolds' stress τ to the other functions. For more complicated flow situations the relation should be extended to a transport equation.[6]

The length scale L is defined as the integral of the two-point space correlations perpendicular to the main stream direction as shown in Fig. 1. It is normalized by the local turbulent energy

$$L = \frac{3}{16E}\int_{-\infty}^{\infty} [\overline{u'(x,y)u'(x,y+r_y)} + \overline{v'(x,y)v'(x,y+r_y)} + \overline{w'(x,y)w'(x,y+r_y)}]\mathrm{d}r_y \tag{5}$$

The transport equation for this quantity has a structure similar to the energy equation and consists again of terms for convection, dissipation, production, and diffusion. Empirical closure assumptions yield

$$\underset{\text{convection}}{\frac{\partial(\bar{u}EL)}{\partial x} + \bar{v}\frac{\partial(EL)}{\partial x}} = \underset{\text{dissipation}}{-cc_L E^{3/2}} + P + \underset{\text{diffusion}}{\frac{k_{qL}}{y^j}\frac{\partial}{\partial y}\left[y^j\sqrt{E}L\left(L\frac{\partial E}{\partial y} + \alpha_L E\frac{\partial L}{\partial y}\right)\right]} \tag{6}$$

Here c_L, k_{qL} and α_L are further coefficients, and P stands for production of the quantity EL.

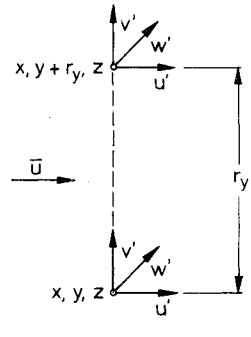

Fig. 1 The definition of two-point correlations and length scale.

When originally derived from the Navier-Stokes equations the production term of this equation reads

$$P = -\frac{3}{16}\frac{\partial \bar{u}}{\partial y}\Big|_y \int_{-\infty}^{\infty} R_{vu}\mathrm{d}r_y - \frac{3}{16y^j}\int_{-\infty}^{\infty}(y+r_y)^j\frac{\partial \bar{u}}{\partial y}\Big|_{y+r_y} R_{uv}\mathrm{d}r_y \tag{7}$$

The definition of the correlations functions

$$R_{vu} = \overline{v'(x,y)u'(u,y+r_y)}$$

and

$$R_{uv} = \overline{u'(x,y)v'(x,y+r_y)}$$

follow from Fig. 1. A Taylor series expansion of the velocity gradient $\partial\bar{u}/\partial y$ under the second integral leads to

$$P = -\frac{\partial \bar{u}}{\partial y}\frac{3}{16}\int_{-\infty}^{\infty}(R_{vu}+R_{uv})\mathrm{d}r_y - \left[\frac{j}{y}\frac{\partial \bar{u}}{\partial y} + \frac{\partial^2 \bar{u}}{\partial y^2}\right]\frac{3}{16}\int_{-\infty}^{\infty} r_y R_{uv}\mathrm{d}r_y - \left[\frac{2j}{y}\frac{\partial^2 \bar{u}}{\partial y^2} + \frac{\partial^3 \bar{u}}{\partial y^3}\right]\frac{3}{32}\int_{-\infty}^{\infty} r_y^2 R_{uv}\mathrm{d}r_y \tag{8}$$

if only the first three terms of the Taylor series are retained. For symmetrical correlation functions R_{uv} (with respect to r_y) the second integral moment in Eq. (8) disappears. Since in the previous investigations (Refs. 6, 7) the asymmetry of R_{uv} was supposed to be negligibly small, the second integral of Eq. (8) was neglected.

The shape of R_{uv} is strongly asymmetric at points where the Reynolds' stress changes sign. Both functions, R_{uv} and R_{vu}, are antisymmetric if the fixed point coincides with the axis or plane of symmetry ($y = 0$). Consequently

$$\int_{-\infty}^{\infty} R_{uv}\mathrm{d}r_y = 0 \tag{9}$$

but

$$\int_{-\infty}^{\infty} r_y R_{uv}\mathrm{d}r_y \neq 0 \tag{10}$$

From these arguments it can be concluded that the first and third terms in Eq. (8) disappear at points where the stress changes sign, while only the second term contributes to the production term. Additionally, from the general relations for the differentiation of the correlation function it follows for $r_y = 0$ and arbitrary y

$$\frac{\partial R_{uv}}{\partial r_y} + \frac{\partial R_{vu}}{\partial y} = \frac{\partial \overline{u'v'}}{\partial y} \tag{11}$$

and – by definition

$$R_{uv} = R_{vu} = \overline{u'v'} \tag{12}$$

These statements suggest, for practical application, a splitting of the correlation function R_{uv} into a symmetric and an antisymmetric part. The symmetric part, $R_{uv}^{(s)}$, is assumed to be proportional to $\overline{u'v'}$, and the antisymmetric part, $R_{uv}^{(a)}$, be proportional to the derivative $\partial\overline{u'v'}/\partial y$. Accordingly, we have the relationship

$$R_{uv} = \overline{u'v'}\,\hat{R}_{uv}^{(s)}\left(\frac{r_y}{L}\right) + \frac{\partial \overline{u'v'}}{\partial y}L\hat{R}_{uv}^{(a)}\left(\frac{r_y}{L}\right) \tag{13}$$

where the dimensionless functions $\hat{R}_{\mu\nu}^{(s)}$ and $\hat{R}_{\mu\nu}^{(a)}$ depend on the dimensionless coordinate r_y/L. Then the production term in Eq. (6) becomes

$$P=\frac{\tau}{\rho}\left\{\zeta\frac{\partial\bar{u}}{\partial y}L+\zeta_3\left[\frac{2j}{y}\frac{\partial^2\bar{u}}{\partial y^2}+\frac{\partial^3\bar{u}}{\partial y^3}\right]L^3\right\}$$

$$+\frac{1}{\rho}\frac{\partial\tau}{\partial y}\zeta_2 L^3\left[\frac{j}{y}\frac{\partial\bar{u}}{\partial y}+\frac{\partial^2\bar{u}}{\partial y^2}\right] \tag{14}$$

where ζ, ζ_2, and ζ_3 are dimensionless coefficients.

It should be noted that the third derivative of $\bar{u}$ in Eq. (14) can be eliminated from Eq. (6). This is achieved by differentiating Eq. (2) with respect to y, after τ has been introduced according to Eq. (4). Therefore, the highest order derivative of $\bar{u}$ in the equation for the length scale is actually of second order.

III. Boundary Conditions

Boundary Conditions Near Walls

The equations (1-4) and (6) do not take into account the influence of the kinematic viscosity on the flowfield near solid walls. Consequently, the exact boundary conditions cannot be satisfied at the surface. The boundary conditions must be defined just outside the viscous regime, which is supposed to be very thin.

Next to the wall, outside the viscous sublayer, the mean velocity profile is described by the logarithmic law of the wall

$$\bar{u}=u_\tau\left(\frac{1}{\kappa}\ln\frac{yu_\tau}{\nu}+C\right) \tag{15}$$

where $u_\tau=\sqrt{\tau_w/\rho}$ is the shear stress velocity, κ von Kármán's constant ($\kappa\approx 0.4$), and C another constant ($C\approx 5.2$).

In the vicinity of the wall the averaged properties of turbulence do not change along streamlines, and the energy diffusion is very small, too. So all but the first two terms on the right hand side of Eq. (3) can be neglected. With Eq. (4), this yields

$$E=\frac{k}{c}L^2\left(\frac{\partial\bar{u}}{\partial y}\right)^2 \tag{16}$$

and

$$\rho E=|\tau|k/c \tag{17}$$

Combination of Eq. (16) and Eq. (17) leads to Prandtl's mixing length formula with the mixing length to be identical to the turbulence scale L. This identification is admissable without prejudice to the definition of Eq. (5), because the equations remain correct, if L is multiplied by an arbitrary factor and the coefficients are properly adjusted at the same time. Furthermore, this leads to the relation

$$c=k^3 \tag{18}$$

which will be used for the determination of k. Finally, we obtain

$$E=(|\tau|/\rho)c^{-2/3} \tag{19}$$

which can be used as a boundary condition for E at a position near the wall.

If the length scale equation is applied to the region of the logarithmic law of the wall, Eq. (15), the convection terms but not the diffusion term are negligible. With the differentiation of Eq. (15), $E=$ const, and the identification of L with the mixing length, i.e. $L=\kappa y$, the relation

$$\zeta-c_L+2\kappa^2\zeta_3+\kappa^2 k_{qL}\alpha_L/c=0 \tag{20}$$

is derived, from which α_L will be determined.

Conditions on Free Boundaries

The free boundaries of turbulent flowfields also need a special treatment. As the viscosity does not appear explicitly in the equations, a line $y_e(x)$ exists which separates the turbulent zone from the region of irrotational flow. The boundary conditions, prescribed for $y=y_e$ are $\bar{u}=u_e(x)$, $E=E_e(x)=0$. No boundary condition is prescribed for L, it is only supposed that L has a finite value, L_e, for $y=y_e$. From Bernoulli's equation is follows

$$\frac{1}{\rho}\frac{\mathrm{d}\bar{p}}{\mathrm{d}x}=-u_e\frac{\mathrm{d}u_e}{\mathrm{d}x}$$

and integration of the continuity equation (1) yields for $y>y_e$

$$v(x,y)=\bar{v}(x,y)=v_e\left(\frac{y_e}{y}\right)^j-\frac{\mathrm{d}u_e}{\mathrm{d}x}\left(y-\frac{y_e^{j+1}}{y^j}\right)\frac{1}{i+j} \tag{21}$$

The differential equations become (inessentially) singular on $y_e(x)$, so that they cannot be treated numerically near that line. It is necessary to investigate the asymptotic behavior of the functions at that region analytically.

For $y<y_e$ and $0<y_e-y\ll 1$ the flow variables may be represented by power series

$$\bar{u}(x,y)=u_e(x)+a(x)\,(y_e(x)-y)^q+\ldots \tag{22a}$$

$$E(x,y)=b(x)\,(y_e(x)-y)^p+\ldots \tag{22b}$$

$$L(x,y)=L_e(x)+\ldots \tag{22c}$$

where the exponents $p>1$ and $q>1$ have to be determined. The approximation of $\bar{v}$

$$\bar{v}(x,y)=\bar{v}_e\left(\frac{y_e}{y}\right)^j-\frac{\mathrm{d}u_e}{\mathrm{d}x}\left(y-\frac{y_e^{j+1}}{y^j}\right)\frac{1}{1+j}$$

$$+a(y_e-y)^q\frac{\mathrm{d}y_e}{\mathrm{d}x}+\ldots \tag{23}$$

can be derived from the continuity equation. As the production and dissipation terms in the energy equations disappear faster with y_e-y than convection and diffusion, we can write

$$\bar{u}\frac{\partial E}{\partial x}+\bar{v}\frac{\partial E}{\partial y}\approx k_q\frac{\partial}{\partial y}\left(\sqrt{E}L\frac{\partial E}{\partial y}\right) \tag{24}$$

This yields with the relations of Eqs. (22)

$$\left(u_e\frac{\mathrm{d}y_e}{\mathrm{d}x}-\bar{v}_e\right)bp(y_e-y)^{p-1}$$

$$=k_q b^{3/2}L_e p\left(\frac{3p}{2}-1\right)(y_e-y)^{[(3p/2)-2]}$$

and it is found that the energy equation is satisfied for $p=2$ and

$$u_e\frac{\mathrm{d}y_e}{\mathrm{d}x}-\bar{v}_e=2k_q\sqrt{b}L_e \tag{25}$$

In the same way the relation

$$u_e\frac{\mathrm{d}y_e}{\mathrm{d}x}-\bar{v}_e=qk\sqrt{b}L_e \tag{26}$$

is derived from the momentum equation (2). By comparison of the relations (25) and (26) the exponent follows from

$$q=2k_q/k \tag{27}$$

By the same arguments the length equation leads again to Eq. (25) with k_{qL} replacing k_q. But the production is negligable only if the condition $q>2$ is satisfied. It is seen that the supposition of a finite vlaue of $L_e(L_e>0)$ requires $k_{qL}=k_q$ and $k_q>k$. These relations are generally used in the calculations.

IV. Similarity Transformation and Numerical Solution

The partial differential equations given in Sec. II were converted into ordinary differential equations by means of similarity transformations. For free turbulent flows the transformations proceed from the known laws of spread (cf. Schlichting[9] or Rotta[7]) and do not include pressure gradients. In this context reference is made also to the work of Görtler[10] and Tollmien.[11] The dependent variables in fully developed flows in channels and pipes are supposed to be independent of the coordinate x.

The ordinary differential equations for mean velocity, kinetic energy of turbulence, and length scale, which have to satisfy boundary conditions on both ends of the interval, were integrated simultaneously, using the so-called shooting technique. The detailed presentation of the transformed equations and the description of the numerical method are given in Ref. 12.

V. Results

The solutions of the equations depend on the choice of the empirical coefficients, occurring in the Eqs. (3, 6 and 14). The main task was, therefore, to determine a single set of the coefficients, which reproduces solutions, which agree with experiments as close as possible for all treated cases. A first estimate resulted from an inductive treatment of the equations, conducted by Rotta.[13] Starting from the values of this study, systematic variations of the coefficients were investigated. The results, which are described in Ref. 13, lead to the following set of coefficients:

$$c=0.165,\ c_L=0.8,\ k_q=0.8,\ \zeta=0.98,\ \zeta_2=1.2$$

$$\zeta_3=-1.5,\ \kappa=0.4,\ k\approx 0.548,\ \alpha_L\approx 0.387$$

This set of coefficients is mainly based on comparisons of mean velocity profiles. The distribution of turbulent energy was only considered for the choice of the value of c. The value $c=0.165$ was already suggested by earlier investigations.[13] It is also supported by the method of Bradshaw, Ferris, and Atwell,[14] where the approximation $\tau=0.3\ \rho E$ is used. The value of c computed from this relation together with Eq. (19) is about that given above.

The distributions of longitudinal mean velocity $\bar{u}$, turbulent energy E and turbulent length, L, calculated with this set of coefficients are plotted with the pertinent similarity coordinates. Experimental values for mean velocity and turbulent energy are indicated by a dashed line. In some cases Prandtl's mixing length is shown as a dash pointed line. In cases of free turbulent flow it is computed by theory as a constant for a flow of half width b given by experiment.

1) The plane free jet emerges from an orifice or a nozzle of high aspect ratio into a resting fluid. Similarity is expected beyond a sufficient distance from the entrance. The profile of $\bar{u}$ in Fig. 2 is compared with measurements by Bradbury.[15]

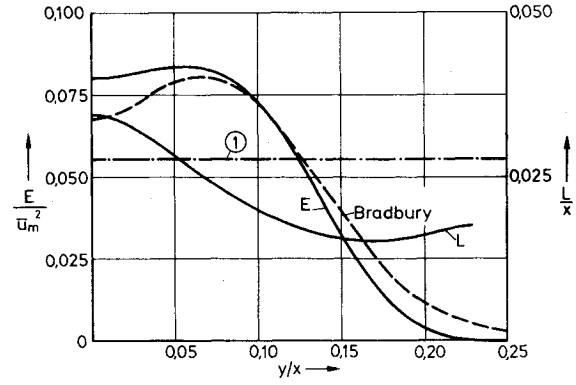

Fig. 3 Profiles of turbulent energy and turbulent length scale of the plane free jet, ① mixing length l/x.

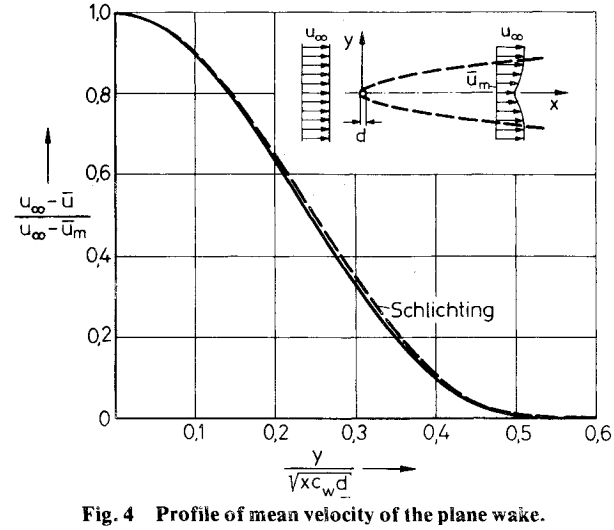

Fig. 4 Profile of mean velocity of the plane wake.

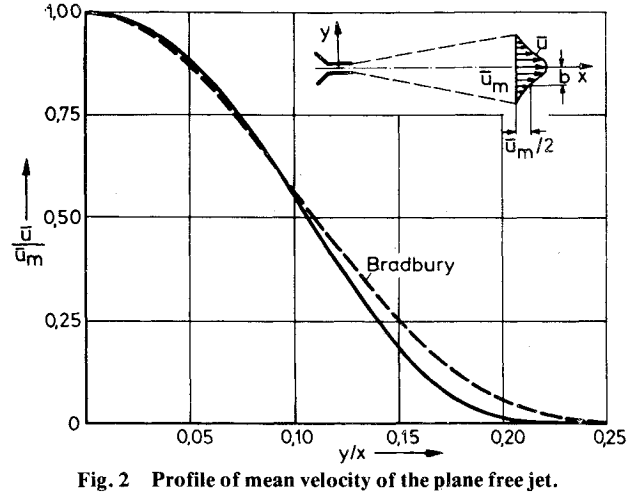

Fig. 2 Profile of mean velocity of the plane free jet.

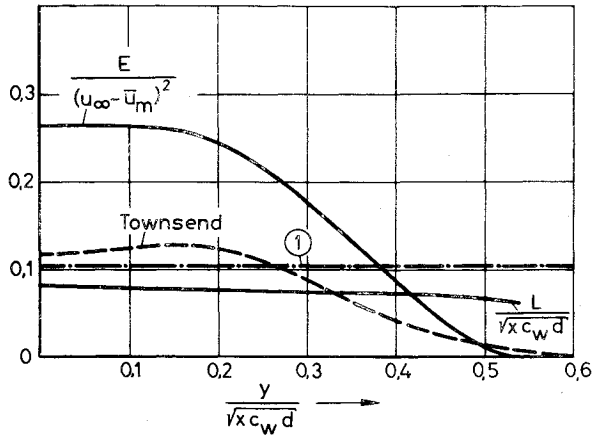

Fig. 5 Profile of turbulent energy and turbulent length scale of the plane wake, ① mixing length $l/\sqrt{xc_w d}$.

The measured half width $b/y=0.11$ deviates only slightly from the computed half width $b/y=0.106$. The energy profiles in Fig. 3 agree satisfactorily. The length L has a maximum in the plane of symmetry and crosses Prandtl's mixing length.

2) The asymptotic plane wake is calculated at a distance x from an assumed circular cylinder of diameter d, where the velocity deficit has decreased to a small fraction of the undisturbed stream ($u_\infty - u_m \ll u_\infty$). Figure 4 shows the velocity deficit $u_\infty - u_m$ as a function of $y/\sqrt{xdc_w}$ where c_w is the drag coefficient normalized with respect to d. The computational value of half width at half maximum, $b/\sqrt{xdc_w}=0.244$, is insignificantly smaller than the experimental value, $b/\sqrt{xdc_w}=0.25$, measured by Schlichting.[16] According to the computation the maximum

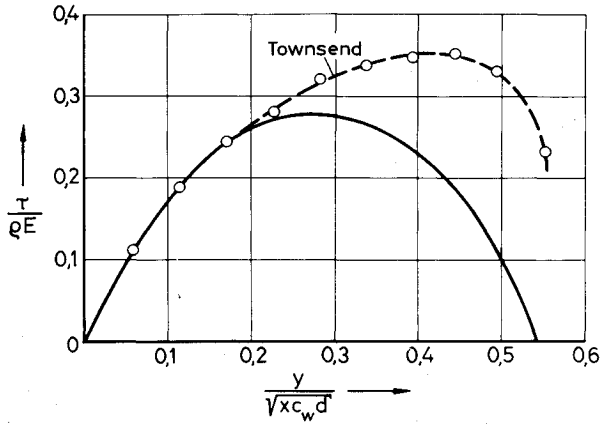

Fig. 6 Ratio $\tau/(\rho E)$ for the plane wake.

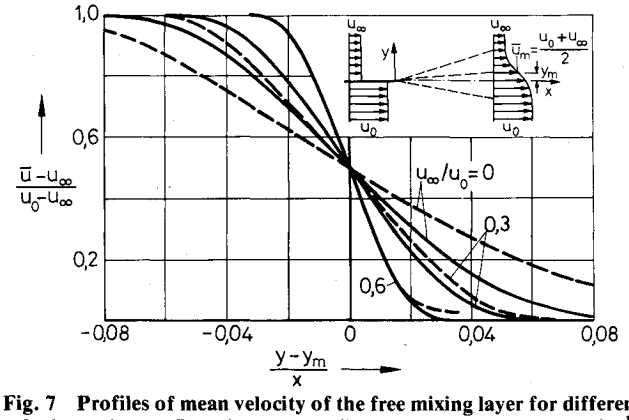

Fig. 7 Profiles of mean velocity of the free mixing layer for different velocity ratios.--- Experimental profiles by Liepmann and Laufer[18] for $u_\infty/u_0=0$ and by Spencer and Jones[19] for $u_\infty/u_0=0.3$ and 0.6.

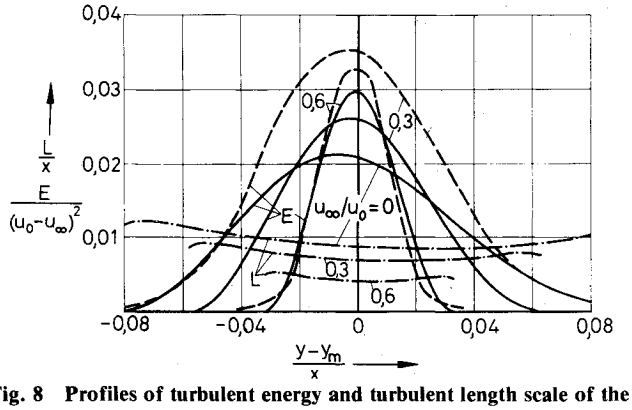

Fig. 8 Profiles of turbulent energy and turbulent length scale of the free mixing layer for different velocity ratios. --- Experimental profiles as for Fig. 7.

Table 1 Comparison of values for spreading of free mixing layers

u_∞/u_0	y_m/y computation	y_m/y experiment
0	0.019	0.03
0.3	0.009	0.02
0.6	0.003	0.005

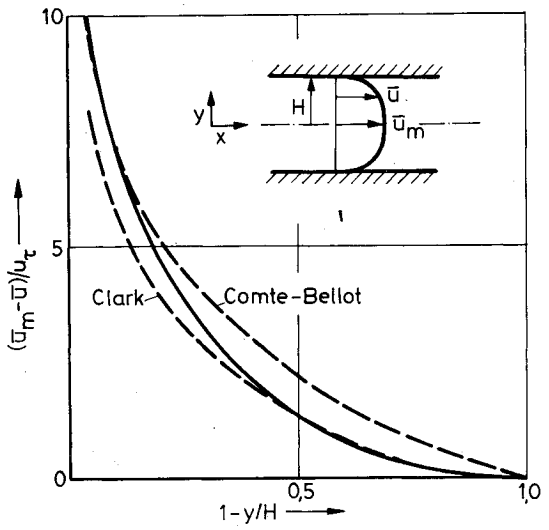

Fig. 9 Profile of mean velocity for the channel flow.

deficit decreases with $u_\infty - u_m = 0.987\sqrt{c_w d/x}$. Significantly greater values for the computed energy than those measured by Townsend[17] are seen in Fig. 5. On the other hand the ratio $\tau/(\rho E)$ extracted from Townsend's measurements[17] is plotted in Fig. 6. It agrees exactly with the computed values in the middle of the wake. Consequently, the measured shear stress is lower than is required by the momentum equation. Thus it is to be concluded, that the experimental data are not compatible with each other. The turbulent length scale, shown in Fig. 5, decreases slightly towards the outer boundary and is smaller than the mixing length.

3) The free mixing layer is created by two coflowing plane jets of different velocities u_∞ and u_0. The profiles of mean velocity, energy, and length are plotted in Figs. 7 and 8 for the velocity ratios $u_\infty/U_0=0$, 0.3 and 0.6. The difference $(y-y_m)/x$, where y_m is the point with $\bar{u}_m=(u_0+u_\infty)/2$, was preferred to y/x as ordinate, because y_m seems to be very sensitive to experimental deviation from the idealized theoretical case. The investigations of Liepmann and Laufer[18] were used for comparison of $u_\infty/u_0=0$ and those of Spencer and Jones[19] for $u_\infty/u_0\neq 0$. For the velocity ratio $u_\infty/u_0=0.6$ the computational results are almost in complete agreement with the experimental data. For lower ratios, the computed spread becomes remarkably lower than the experimental one and, accordingly, the turbulent energy is too low. The length scale varies only slightly with y. Experimental and computed values of y_m/x are compared in Table 1.

4) The fully developed flow through a channel of half-height H and high aspect ratio is supposed to be two-dimensional. The velocity profiles $\bar{u}$ is presented as law of the center in Fig. 9. Clark's measurements[20] for $Re=1.3\cdot 10^5$‡ coincide with the computational results. The experiments of Comte-Bellot[21] for $Re=2.3\cdot 10^5$ show a less full profile. Figure 10 demonstrates the good agreement of turbulent energy in the center. Possible reasons for the increasing differences towards the wall are discussed in connection with the results of the pipe flow. The length scale deviates remarkably from its asymptote lim $L=0.4\,(H-y)$ already at

‡$Re=2UH/\nu$, U velocity averaged over the cross section.

small distances from the wall. It has the value $L/H \approx 0.25$ at the center line.

5) The axisymmetric jet emerges from a circular hole or nozzle into a resting fluid and is the counterpart of the plane jet. The computational results are compared with experimental data of Wygnanski and Fiedler.[22] The profiles of the longitudinal velocity in Fig. 11 differ only slightly. The computational half width $b/x = 0.0894$ has to be compared

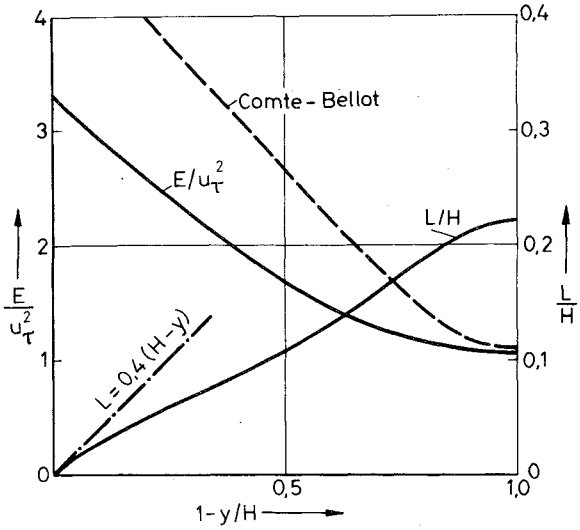

Fig. 10 Profiles of turbulent energy and turbulent length scale for the channel flow.

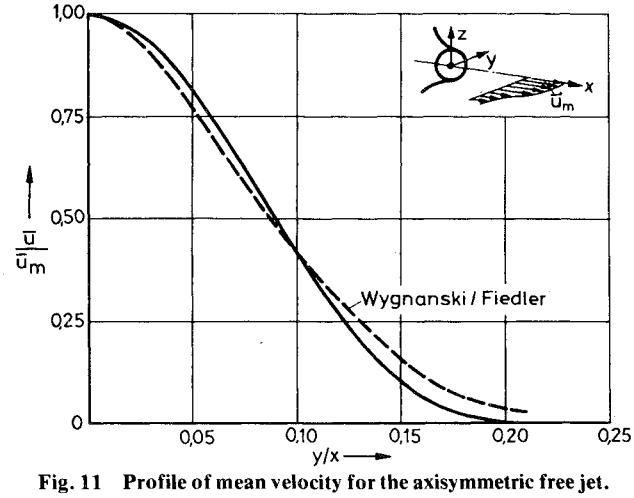

Fig. 11 Profile of mean velocity for the axisymmetric free jet.

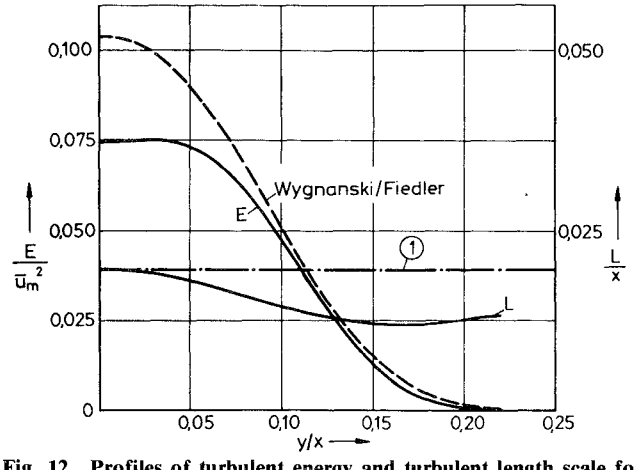

Fig. 12 Profiles of turbulent energy and turbulent length scale for the axisymmetric free jet, ① mixing length.

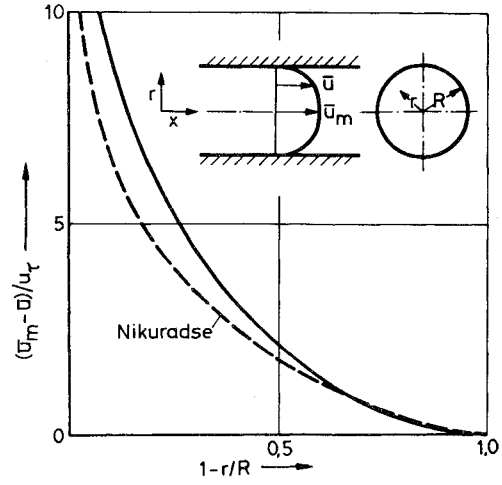

Fig. 13 Profile of mean velocity for the pipe flow.

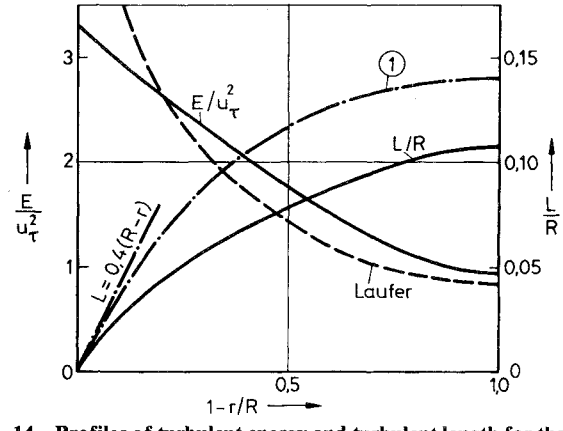

Fig. 14 Profiles of turbulent energy and turbulent length for the pipe flow, ① mixing length l, $l/R = 0.14 - 0.08\,(r/R)^2 - 0.06\,(r/R)^4$.

with the experimental value $b/x = 0.088$. The energy profiles in Fig. 12 nearly coincide for $y/x > 0.9$. In the center the computed values are considerably lower than the measured ones. The length scale distribution has the same shape as that for the plane jet, though it is essentially smaller. The mixing length is higher than the average value of L/x.

6) For the fully developed flow through a circular pipe of radius R the situation is similar to the channel flow. The computed mean velocity profile in Fig. 13 is slightly too peaked compared to measurements of Nikuradse[23] at Reynolds numbers $Re \geq 10^5$§. The comparison of Laufer's data[24] at $Re = 5 \cdot 10^5$§ with the computed energy profiles in Fig. 14 shows satisfactory agreement near the center and increasing differences towards the wall. This deviation can be understood from the fact, that turbulent motion near the wall presumably consists of two parts: An 'active' part which produces the stress and 'inactive' part generated by motion far from the wall.[25] Although the 'inactive' fluctuations can reach rather high values they practically do not affect the mean velocity profile. As they are not included in the used equations they are probably responsible for the discrepancy of the energy profiles. The length scale has a similar shape as the mixing length determined by Nikuradse[23] but it is smaller and deviates strongly from its asymptote $\lim_{y \to R} L = 0.4\ (R - r)$ already near the wall. The value in the center is only half of that for the plane channel

VI. Conclusions

A system of partial differential equations for the description of turbulent flowfields was treated. It consists of

§ $Re = 2UR/\nu$, U velocity averaged over the cross section.

Table 2 Range of boundary conditions

	plane flow	axisymmetric flow
free flows	free jet ($u_\infty = 0$) wake ($u_\infty - \tilde{u}_m \ll u_\infty$) free mixing layer ($u_\infty / u_0 = 0, 0.3, 0.6$)	free jet ($u_\infty = 0$)
flows with walls	channel flow	pipe flow

relations between the mean velocity components, the Reynolds' stress, the kinetic turbulent energy and the characteristic length scale which is defined as an integral of second-order correlations. By assuming similarity of the flow quantities the equations were transformed into ordinary differential equations. They were solved numerically for six different turbulent flowfields. The wide range of boundary conditions of the treated cases is illustrated in Table 2.

The influence of the empirical coefficients on the solutions was investigated by systematic variations.

As the most important result of the investigations, a single set of coefficients was determined. The calculated results, obtained with this set of coefficients display, generally speaking, fair agreement with the experiments.

Since the decay of homogeneous turbulence is well approximated, too, the system of equation seems to describe correctly the essentials of the mechanism of turbulence. But according to the strong simplifications of the equations, it is not surprising that an exact quantitative description could not be achieved.

Acknowledgment

This research was supported by the Deutsche Forschungsgemeinschaft.

References

[1]Bradshaw, P., "The Understanding and Prediction of Turbulent Flow," Sixth Reynolds-Prandtl Lecture, *Aeronautical Journal*, Vol. 76, 1972, pp. 403-418.

[2]Mellor, G. L. and Herring, H. J., "A Survey of the Mean Turbulent Field Closure Models," *AIAA Journal*, Vol. 11, May 1973, pp. 590-599.

[3]Launder, B. E., Spalding, D. B., *Mathematical Models of Turbulence*, Academic Press, London, 1972.

[4]Rotta, J. C., "Turbulent Shear Layer Prediction on the Basis of the Transport Equations for the Reynolds Stresses," *Proceedings of the 13th Congress of Theoretical and Applied Mechanics*, Moscow 1972, pp. 295-308, E. Becker and G. K. Mikhailow (eds.), Springer-Verlag Berlin/Heidelberg/New York, 1973.

[5]Reynolds, W. C., "Computations of Turbulent Flows," *Annual Review of Fluid Mechanics*, Vol. 8, 1976, pp. 183-208.

[6]Rotta, J. C., "Recent Attempts to Develop a Generally Applicable Calculation Method for Turbulent Shear Flow Layers," AGARD CP No. 93, 1972.

[7]Rotta, J. C., *Turbulente Strömungen*, Verlag B. G. Teubner, Stuttgart, 1972.

[8]Prandtl, L., "Ueber ein neues Formelsystem für die ausgebildete Turbulenz," *Nachrichten der Akademie der Wissenschaften Göttingen*, Math. Phys. K1, 1945, pp. 6-19.

[9]Schlichting, H., *Boundary-Layer Theory*, McGraw-Hlll, New York, 1968.

[10]Görtler, H., "Berechnung von Aufgaben der freien Turbulenz auf Grund einers neuen Näherungsansatzes," *Zeitschrift für Angewandte Mathematik und Mechanik*, Vol. 22, 1942, pp. 244-254.

[11]Tollmien, W., "Berechnung turbulenter Ausbreitungsvorgänge," *Zeitschrift für Angewandte Mathematik und Mechanik*, Vol. 6, 1926, pp. 468-478.

[12]Rotta, J. C., Vollmers, H., "Aehnliche" Lösungen der Differentialgleichungen für gemittelte Geschwindigkeiten, Turbulenzenergie und Turbulenzlänge, DLR-FB 76-24, 1976.

[13]Rotta, J. C., "Induktive Behandlung des Prandtlschen Formelsystems für die ausgebildete Turbulenz von 1945," DLR-FB 74-51, 1974, pp. 1-39.

[14]Bradshaw, P., Ferriss, D. H., Atwell, P. N., "Calculation of Boundary-Layer Development Using the Turbulent Energy Equation," *Journal of Fluid Mechanics*, Vol. 28, 1967, pp. 593-616.

[15]Bradbury, L. J. S., "The Structure of a Self-Preserving Turbulent Plane Jet," *Journal of Fluid Mechanics*, Vol. 23, 1965, pp. 31-64.

[16]Schlichting, H., "Ueber das ebene WindschattenProblem, *Ingenieur-Artchiv*, Vol. 1, 1930, pp. 533-571.

[17]Townsend, A. A., *The Structure of Turbulent Shear Flow*, Cambridge Univ. Press., Cambridge, England, 1956.

[18]Liepmann, H. W., Laufer, J., "Investigations of Free Turbulent Mixing," NACA TN 1257, 1947.

[19]Spencer, B. W., Jones, B. G., "Statistical Investigation of Pressure and Velocity Fields in the Turbulent Two-Stream Mixing Layer," AIAA Paper 71-613, Palo Alto, Calif., 1971.

[20]Clark, J. A., "A Study of Incompressible Turbulent Boundary Layers in Channel Flow," *Journal of Basic Engineering*, Vol. 90, 1968, pp. 455-467.

[21]Comte-Bellot, G., "Ecoulement turbulent entre deux parois paralleles," Publ. Sci. Techn. du Ministere de l'Air, No. 419, 1965.

[22]Wygnanski, I., and Fiedler, H. E., "Some Measurements in the Self-Preserving Jet," *Journal of Fluid Mechanics*, Vol. 38, 1969, pp. 577-612.

[23]Nikuradse, J., "Gesetzmässigkeiten der turbulenten Strömungen in glatten Rohren," VDI-Forschungsheft 356, 1932, pp. 1-36.

[24]Laufer, J., "The Structure of Turbulence in Fully Developed Pipe Flow," NACA TR 1174, 1954.

[25]Bradshaw, P., "Inactive Motion and Pressure Fluctuations in Turbulent Boundary Layers," *Journal of Fluid Mechanics*, Vol. 30, 1967, pp. 241-258.